

POTENTIAL MICROENCAPSULATION OF PYRITE BY ARTIFICIAL INDUCEMENT OF FePO_4

COATINGS

V.P. Evangelou

Abstract: A novel coating methodology was developed to prevent pyrite oxidation in mining "waste." The mechanism of this coating technology involves leaching mining "waste" with a phosphate solution containing hydrogen peroxide (H_2O_2); when this solution reaches pyrite surfaces, H_2O_2 oxidizes the surface portion of pyrite and releases Fe^{3+} so that iron phosphate precipitates and forms a passive coating on pyritic surfaces. This study demonstrated that iron phosphate coatings on pyritic surfaces could be established with a solution containing as low as 10^{-4} mol/L phosphate and 0.027 mol/L H_2O_2 and that the iron phosphate coating could effectively protect pyrite from oxidizing further. Development of this coating methodology could mean solution to production of acid mine drainage from certain types of mine "waste." Further investigations are being carried out to extend this methodology to practical use.

Introduction

Pyrite oxidation in mining "waste" or overburden is considered as the main cause for the production of acid mine drainage (AMD). The need to prevent AMD formation has triggered numerous investigations into the mechanisms of pyrite oxidation and its prevention (Singer and Stumm, 1970; Silverman, 1967; Nordstrom, 1982; Kleinmann et al., 1981; Ziemkiewicz, 1990).

It has been reported that pyrite in mining wastes or coal overburden is initially oxidized by the atmospheric O_2 , producing H^+ , SO_4^{2-} , and Fe^{2+} (Nordstrom, 1982). The Fe^{2+} produced can be further oxidized by O_2 into Fe^{3+} , which in turn hydrolyzes into amorphous iron hydroxide and releases additional amounts of acid into the environment (Nordstrom, 1982). In this initial stage, pyrite oxidation in pyritic "waste" is a relatively slow process (Ivanov, 1962). As acid production continues and the pH in the vicinity of the pyritic surfaces drops below 3.5, the formation of ferric oxide is hindered and the activity of free Fe^{3+} in solution increases. Under these conditions, the oxidation of pyrite by Fe^{3+} becomes the main mechanism for acid production in mining wastes since Fe^{3+} can oxidize pyrite at a much faster rate than O_2 (Singer and Stumm, 1970). Meanwhile, at low pH, an acidophilic, chemoautotrophic, iron-oxidizing bacterium, *Thiobacillus ferrooxidans*, flourishes; it can catalyze and accelerate the oxidation of Fe^{2+} into Fe^{3+} by a factor larger than 10^6 (Singer and Stumm, 1970) and thereby effectively recycle the iron released from pyrite as a major oxidant of pyrite or as an electron conductor between FeS_2 and O_2 (Kleinmann et al., 1979). *Thiobacillus ferrooxidans* is thus considered to be primarily responsible for the rapid oxidation of pyrite in mining wastes at low pH (Nordstrom, 1982).

So far the approaches to preventing pyrite oxidation are mainly based on the above mechanisms and are aimed at eliminating Fe^{3+} from pore waters. These approaches include the use of phosphate to precipitate Fe^{3+} in the insoluble form as FePO_4 (Ziemkiewicz, 1990) and the application of bactericides to inhibit the oxidation of Fe^{2+} into Fe^{3+} (Kleinmann et al., 1981). Both approaches have shown a certain degree of success in preventing pyrite oxidation and acid production in pyritic "waste"; however, they both have two weaknesses—they are costly and have a short span of effectiveness. The main reason for the failure of these methods is that the surfaces of pyrite particles in mining "waste" are still exposed to the atmospheric O_2 after treatment; as Fe^{2+} accumulates and *Thiobacillus ferrooxidans* repopulates on pyritic surfaces, pyrite oxidation by Fe^{3+} and acid production is initiated (Kleinmann and Crerar, 1979). To completely prevent pyrite oxidation, it appears essential to block the access of the atmospheric O_2 to pyritic surfaces.

The purpose of this study was to examine the feasibility of creating an iron phosphate coating on pyrite surfaces to prevent pyrite oxidation. The basic hypothesis for this coating approach was that by leaching pyritic mining "waste" with a phosphate solution containing a low concentration of H_2O_2 , the Fe^{3+} released from pyrite by H_2O_2 will react with phosphate to form a passive FePO_4 coating on pyrite surfaces. Thus, at the expense of a small fraction of pyrite, oxidation of pyrite and production of acid could be prevented.

Theory

Pyrite Oxidation by H_2O_2

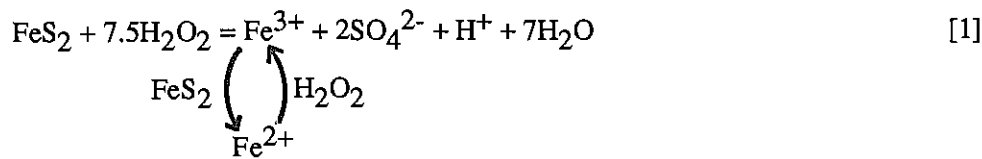
Pyrite oxidation by H_2O_2 can be described as follows (Huang and Evangelou, 1992):

Paper presented at the International Land Reclamation and Mine Drainage Conference and the Third International Conference on the Abatement of Acidic Drainage, Pittsburg, PA, April 24-29, 1994.

V. P. Evangelou, Department of Agronomy, Univ. of Kentucky, Lexington, KY 40546-0091.

Proceedings America Society of Mining and Reclamation, 1994 pp 96-103

DOI: 10.21000/JASMR94020096



According to equation 1, pyrite oxidation is an autocatalytic process because one of the oxidation products, Fe^{3+} , can also oxidize pyrite. The rate law corresponding to this oxidation mechanism can be written as

$$-dM/dt = (k_1[\text{H}_2\text{O}_2] + k_2[\text{Fe}^{3+}])KM, \quad [2]$$

where M is the number of moles of pyrite in the system at any time t. $[\text{H}_2\text{O}_2]$ and $[\text{Fe}^{3+}]$ refer to concentrations of H_2O_2 and Fe^{3+} , while k_1 and k_2 refer to the rate constants of H_2O_2 and Fe^{3+} , respectively; K stands for the specific surface of pyrite.

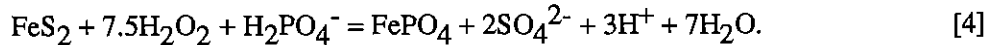
By moving M in equation 2 to the left-hand side, integrating with respect to M and expressing it as log to the base 10, equation 2 becomes

$$-\text{dlog}M/dt = (k_1/2.3[\text{H}_2\text{O}_2] + k_2/2.3[\text{Fe}^{3+}])K. \quad [3]$$

According to equation 3, the first-order plot of log M versus t will be curvilinear even if $[\text{H}_2\text{O}_2]$ is kept constant. Whether the plot concaves down or up depends on whether the Fe^{3+} concentration in the system increases or decreases with time. However, if Fe^{3+} is prevented from oxidizing pyrite and $[\text{H}_2\text{O}_2]$ is kept constant, the plot will be a straight line.

Pyrite Oxidation by H_2O_2 in the Presence of Phosphate

Pyrite oxidation by H_2O_2 in the presence of phosphate can be described by:



The iron phosphate formed can precipitate either as a discrete phase or as a coating on pyritic surfaces, depending on the degree of the supersaturation of the solution on pyritic surfaces with respect to iron phosphate (Huang and Evangelou, 1992). If the degree of supersaturation is relatively low, the iron phosphate might not precipitate instantly and thereby exist as a discrete phase. In this case, equation 3 becomes

$$-\text{dlog}M/dt = Kk_1/2.3[\text{H}_2\text{O}_2]. \quad [5]$$

This equation implies that the precipitation of iron phosphate as a discrete phase is characterized by the linear first-order plot of log M versus t if $[\text{H}_2\text{O}_2]$ is kept constant.

If the degree of supersaturation with respect to iron phosphate is high, iron phosphate will precipitate as a coating on pyritic surfaces. The rate of pyrite oxidation should be smaller than that predicted by equation 5 as pyrite oxidation is not only surface chemical reaction-controlled but also coatings-controlled. In this case, the kinetics of pyrite oxidation would be described by the shrinking core model (Huang and Evangelou, 1992; Nicholson et al., 1989):

$$t = 1/(D_s'C)\{1 - 3(1-X)^{2/3} + 2(1-X)\} + 1/(K_s'C)\{1 - (1-X)^{1/3}\} \quad [6]$$

where t is the time required for a specific fraction (X) of pyrite to oxidize in the system and C is the concentration of H_2O_2 in the bulk solution. D_s' is the apparent diffusion coefficient for H_2O_2 through FePO_4 coatings and K_s' is the first-order rate constant with respect to pyrite. The first term in equation 6 describes the effect of accumulation of iron phosphate precipitates on pyritic surfaces on the rate of pyrite oxidation. The second term describes the first-order kinetics with respect to pyrite itself. Note: The second term in equation 6 is the same as equation 5.

Materials and Methods.

The sample used in this study was a pyritic shale with 6.5% pyrite. The shale sample was pulverized, passed through a 60-mesh sieve, and stored in a plastic bag. Part of the pulverized sample was used to separate pyrite using a heavy liquid, 97% tetrabromoethane. The separated pyrite particles were washed with 4 mol/L hydrofluoric acid to remove silicate and iron oxides and then rinsed repeatedly with nitrogen-purged distilled water. The cleaned sample

was then dried and stored in a vacuumed desiccator. X-ray diffraction analysis indicated that the separated sample was pure pyrite and free of any crystalline impurities.

To prove the feasibility of coating pyrite with iron phosphate, we leached a mixture of 50 mg of the separated pyrite sample and 500 mg of 140-mesh sand with the following three solutions, using a chromatographic column (fig. 1) and a peristaltic pump at a flow rate of 0.5 mL/min and a temperature of 40°C: 0.147 mol/L H_2O_2 , 0.147 mol/L H_2O_2 with 0.013 mol/L disodium ethylenediamine tetraacetate (EDTA), 0.147 mol/L H_2O_2 with 0.01 mol/L KH_2PO_4 . All three solutions contained 0.1 mol/L NaCl as background electrolyte and were adjusted to pH 4 with 0.01 mol/L HCl. At pH 4, it was expected that the Fe^{3+} produced during pyrite oxidation was either completely complexed by EDTA or precipitated by phosphate as $FePO_4$. The pyrite-sand mixture in the column was pressed into a disc with a diameter of 10 mm and a thickness of 3 mm and preleached with 50 mL of 2 mol/L HCl to guarantee removal of free $FeSO_4$ and iron oxides. The leachate from the column was collected at 20-min. intervals with a fraction collector.

At the end of leaching, the residual pyrite particles in the pyrite-sand mixture were separated with 97% tetrabromoethane. The residual pyrite particles were further washed with acetone and dried in a vacuumed desiccator. The surface status of pyrite particles was then examined using scanning electron microscopy and diffuse reflectance infrared spectroscopy.

To determine the effectiveness of the coating approach in preventing pyrite oxidation, two columns with a mixture of 0.5 g of the pulverized shale and 0.5 g of 140-mesh sand were leached first with 50-mL of 2 mol/L HCl to expose pyritic surfaces and then with 500-mL of pH 4 solutions containing 0.1 mol/L NaCl, 10^{-4} mol/L KH_2PO_4 , and 0.053 mol/L H_2O_2 to coat pyrite particles. The leachates were collected in a 500-mL bottles. One of the columns was leached again with 50 mL of 2 mol/L HCl to remove the iron phosphate coating. Both columns were then subjected to leaching at 40°C with a pH 4 oxidizing solution containing 0.1 mol/L NaCl and 0.088 mol/L H_2O_2 to test the effectiveness of the coating in preventing pyrite oxidation. Leachates were collected at 20-min intervals using a fraction collector. All the leaching experiments were conducted using the chromatographic column (fig. 1) at 40°C and a flow rate of 0.5 mL/min.

Sulfate concentration in the leachates was measured using turbidometry with $BaCl_2$. The amount of pyrite remaining in the column was calculated according to the FeS_2-SO_4 stoichiometry and the extent of pyrite oxidation was expressed as percent of remaining pyrite versus time.

Results and Discussion

Kinetics of Pyrite Oxidation During Leaching

Figure 2 shows the first-order plot of $\log(100 \times M/M_0)$ versus t (M_0 = original amount of pyrite, and M = amount of unreacted pyrite at any time t) for the data of pyrite oxidation when pyrite was leached with the three solutions listed in the caption. During leaching with 0.147 mol/L H_2O_2 , pyrite rapidly oxidized and by the end of leaching, 70% of pyrite was oxidized. The first order plot was curvilinear and concaved up. Since the total volume of pores in the pyrite-sand column was small (the total volume of the column was 0.058 cm^3), the concentration of H_2O_2 used was high, and the residence time of the leaching solution within the column was low, it was assumed that H_2O_2 concentration in contact with pyritic surfaces was always constant. With this assumption, the curvature of the first order plot can be attributed to oxidation of pyrite by Fe^{3+} (equation 3). The analysis of the iron in the leachate indicated that the amounts of the soluble Fe^{3+} released from pyrite decreased dramatically with time, and approximately 50% of iron released from pyrite precipitated as iron hydroxide within the column by the end of leaching (fig. 3A).

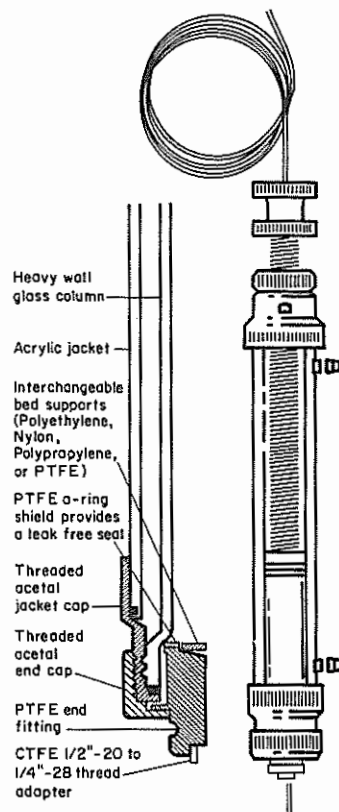


Figure 1. Chromatographic column for pyrite leaching experiments.

When pyrite was leached with the solution containing 0.147 mol/L H_2O_2 and 0.013 mol/L EDTA, the rate of pyrite oxidation decreased, especially during the initial stage of leaching, but it did not stop; at the end of leaching, approximately 65% of pyrite was oxidized, a value close to that for being leached with 0.147 mol/L H_2O_2 . The first order plot was a straight line (fig. 2, curve B). This indicated that pyrite oxidation by Fe^{3+} had been completely inhibited by EDTA (equation 3). Analysis of iron in the leachates confirmed that 100% of the iron released from pyrite was instantly flushed out of the column (fig. 3, curve B).

When the pyrite was leached with the solution containing 0.147 mol/L H_2O_2 and 10^{-2} mol/L KH_2PO_4 , almost 99% of the iron released from the pyrite was precipitated by phosphate (fig. 3, curve C). The precipitation of iron as $FePO_4$ might influence the rate of pyrite oxidation via two mechanisms: (1) by inhibiting the oxidation of pyrite by Fe^{3+} or (2) by forming a passive coating. As shown in figure 2, pyrite oxidation during leaching with the solution containing 0.147 mol/L H_2O_2 and 0.01 mol/L KH_2PO_4 was much slower than that during leaching with the solution containing 0.147 mol/L H_2O_2 and 0.013 mol/L EDTA (fig. 2, curve C). Before 300 min, the first-order plot was nearly parallel to that of EDTA treatment. This indicates that at the initial stage of leaching phosphate inhibited oxidation of pyrite by Fe^{3+} by precipitating Fe^{3+} as $FePO_4$, but not all the iron phosphate had precipitated as coating. After 300 min of leaching, pyrite oxidation nearly stopped. At the end of leaching, more than 70% of pyrite was preserved. The above results clearly suggest that by leaching with the phosphate solution containing H_2O_2 , we can establish an iron phosphate coating on pyrite surfaces at the expense of surface portions of pyrite particles.

The growth of iron phosphate coatings on pyrite surfaces during leaching with phosphate solution containing H_2O_2 can be well explained with the shrinking core model. As indicated in the Theory section, the second term in equation 6 represents first-order kinetics with respect to pyrite. During leaching with the solution containing H_2O_2 and EDTA, pyrite oxidation by Fe^{3+} was inhibited and no coatings were supposed to form. Thus, the rate of pyrite oxidation by H_2O_2 is of the first order with respect to pyrite. This was clearly confirmed by the linearity of the plot of t versus $\{1-(1-X)^{1/3}\}$ (fig. 4) (deviation from straight line at around 700 min is believed to be due to the failure of the linear relationship between the surface area and the mole number of the remaining pyrite (Turner, 1960)). With the apparent first-order rate constant obtained from the plot in figure 4, we expressed the data of pyrite oxidation during leaching with the solution containing 0.147 mol/L H_2O_2 and 0.01 mol/L KH_2PO_4 as a plot of $t-1/(Ks'C)\{1-(1-X)^{1/3}\}$ versus $\{1-3(1-X)^{2/3} + 2(1-X)\}$ (fig. 5). The values of $t-1/(Ks'C)\{1-(1-X)^{1/3}\}$ represent the extra time required for H_2O_2 to oxidize a given fraction of pyrite due to iron phosphate coatings. As shown in figure 5, the plot followed a straight line after 200 min of leaching. The shrinking model requires that all the iron phosphate formed precipitate as a coating on pyritic surfaces. The deviation from linearity before 200 min indicates that some iron phosphate did not precipitate as coating. Part of the reason is that the concentration of acid produced by pyrite oxidation was relatively high during the initial stages of leaching (pH of the leachates was 2.7 in the first 200 min of leaching). The acid

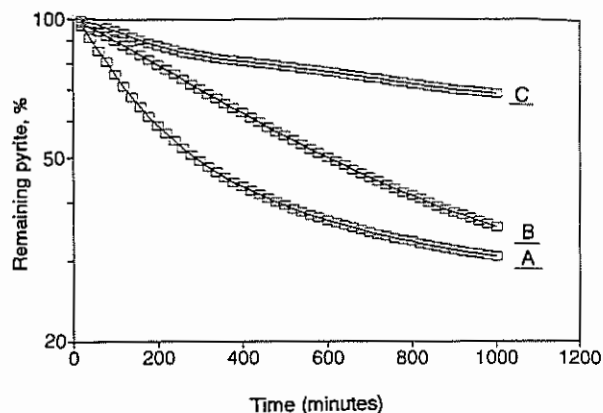


Figure 2. The first-order plot of $\log(100 \times M/M_0)$ versus t for the data of pyrite oxidation when pyrite was leached with the following three solutions: A, 0.147 mol/L H_2O_2 ; B, 0.147 mol/L H_2O_2 plus 0.013 mol/L EDTA; C, 0.147 mol/L H_2O_2 plus 0.01 mol/L KH_2PO_4 .

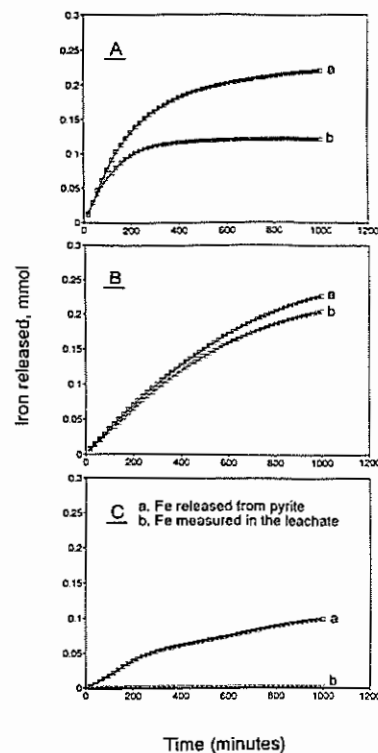


Figure 3. Release of iron as calculated according to the $Fe-SO_4$ stoichiometry and as measured in the leachates when pyrite was leached with the solutions listed in figure 2.

can inhibit formation of iron phosphate coatings owing to its influence on the degree of supersaturation with respect to FePO_4 and thereby increase the amount of pyrite oxidized to create iron phosphate coatings. The use of a buffer reagent will greatly decrease the amount of pyrite oxidized to create the coating.

Surface Analysis

Scanning electron microscope photos show that after leaching with 0.147 mol/L H_2O_2 , the residual pyrite particles were coated with a layer of iron hydroxide. But the framboidal morphology of most pyrite particles were still distinguishable (fig. 6A). This indicates that iron hydroxide did not precipitate as a coating owing to its relatively high solubility, although 0.1 mol of iron hydroxide formed during leaching within the column. As expected, the residual pyrite particles leached with the solution containing 0.147 mol/L H_2O_2 and 0.013 mol/L EDTA were free of any coatings (fig. 6B). Most pyrite particles displayed a typical framboidal morphology. Nevertheless, after leaching with the solution containing 0.147 mol/L H_2O_2 and 0.01 mol/L KH_2PO_4 , residual pyrite particles were so heavily coated with FePO_4 that crystals constituting pyrite particles were barely identifiable (fig. 6C). In addition, pyrite particles were much smaller than was observed for residual pyrite particles after leaching with H_2O_2 or H_2O_2 plus EDTA. This indicates that leaching with the phosphate solution containing H_2O_2 will introduce an iron phosphate coating on any size of pyrite particles.

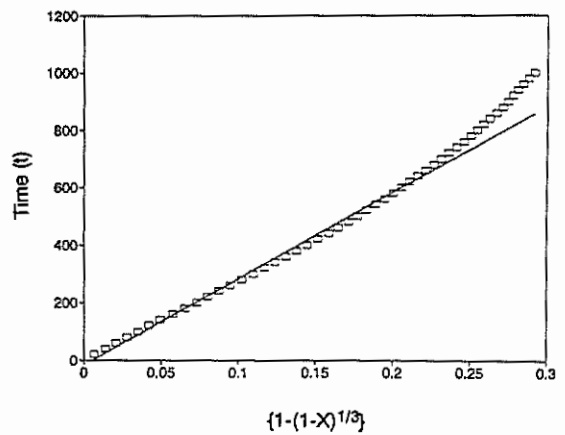


Figure 4. A model plot of t versus $\{1-(1-X)^{1/3}\}$ for the data of pyrite oxidation during leaching with the solution containing 0.147 mol/L H_2O_2 and 0.013 mol/L EDTA.

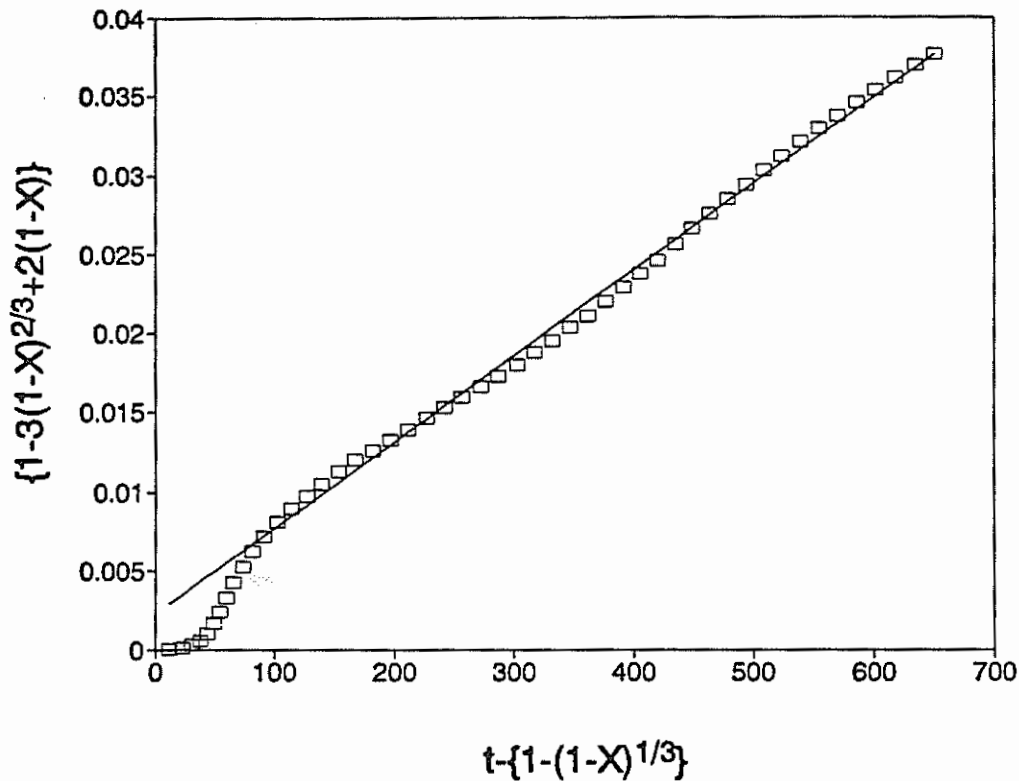


Figure 5. A model plot of $\{1-3(1-X)^{2/3}+2(1-X)\}$ versus $t\{1-(1-X)^{1/3}\}$ for the data of pyrite oxidation during leaching with the solution containing 0.147 mol/L H_2O_2 and 0.01 mol/L KH_2PO_4 .

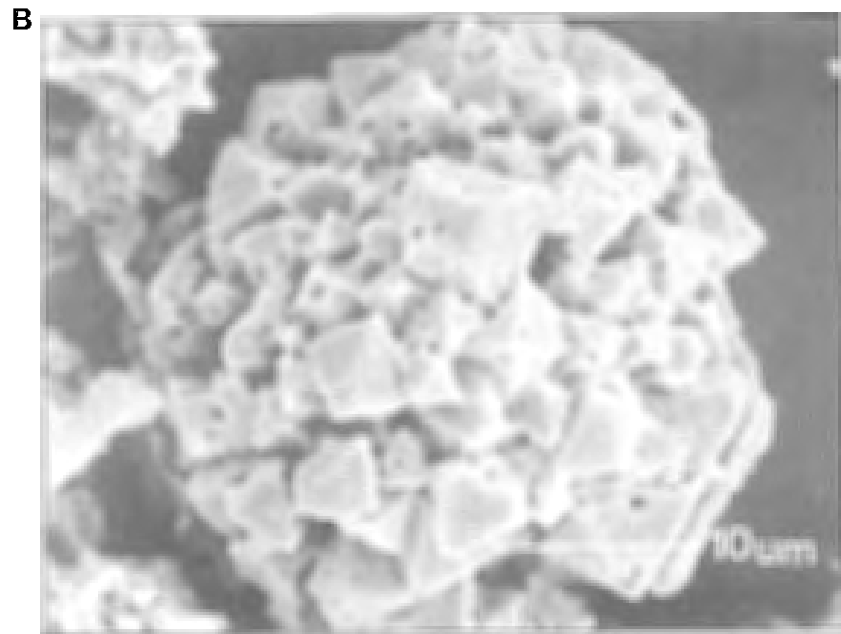
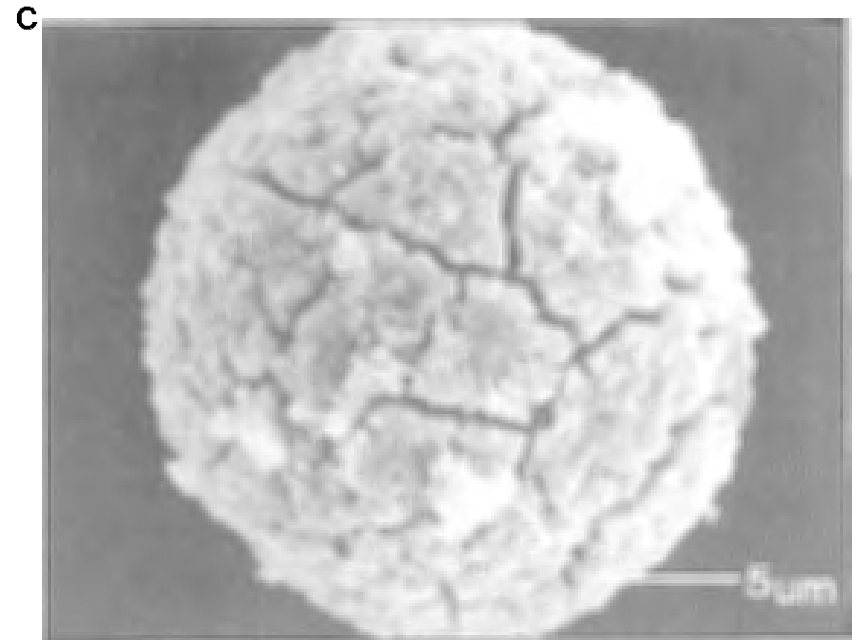
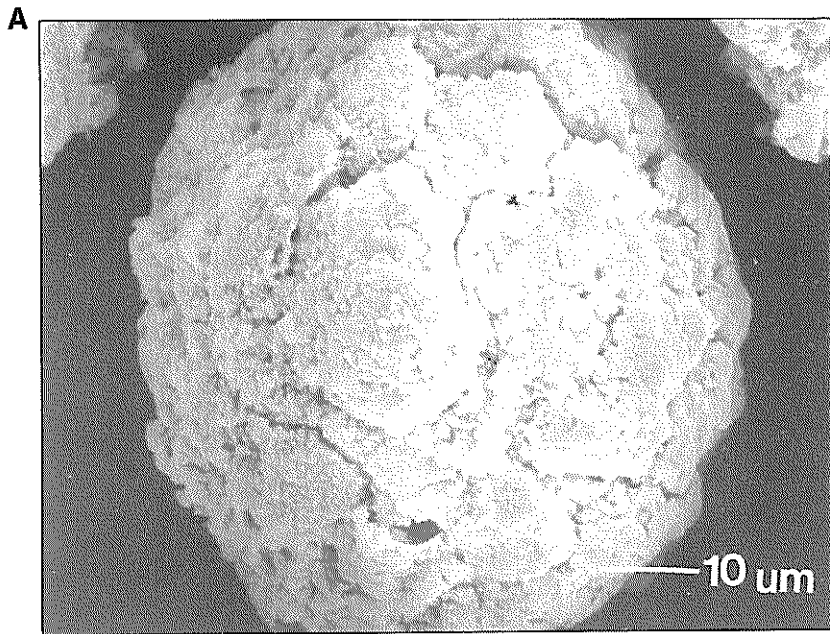


Figure 6. Scanning electron microscope photos showing the surface status of pyrite particles after leaching with **A**, 0.147 mol/L H_2O_2 ; **B**, 0.147 mol/L H_2O_2 plus 0.013 mol/L EDTA; **C**, 0.147 mol/L H_2O_2 plus 0.01 mol/L KH_2PO_4 .

Considering an FePO_4 precipitate of 0.1 mol with an FePO_4 gravity density of 2.73 g cm^{-3} and a pyrite specific surface of $7.3 \text{ m}^2/\text{g}$, its thickness was estimated to be approximately 188 Å (assuming that all the iron phosphate was precipitated as coating). Although the coating appears to be thin, the results in figure 2 indicate that once the coating was established H_2O_2 in the coating solution could no longer attack pyrite, and that iron phosphate coating was an effective H_2O_2 -diffusion inhibitor.

To further understand the chemical properties of the iron phosphate coating, we repeated the leaching experiment with two columns of pure pyrite (50 mg pyrite and 500 mg sand) and the solution containing 0.147 mol/L H_2O_2 and 0.01 mol/L KH_2PO_4 . At the end of leaching, one column continued to be leached with 50 mL of 2 mol/L HCl . The leachate was analyzed for iron and phosphate. We found out that the mole ratio of iron to phosphate was 1.0, indicating that the coating was FePO_4 and no hydroxyl entered the structure of iron phosphate. The pyrite in the other column was separated from the pyrite-sand mixture and its surface was examined using diffuse reflectance infrared spectroscopy (FT-IR). As shown in figure 7 (curve A), after leaching with the solution containing 0.147 mol/L H_2O_2 and 10^{-2} mol/L KH_2PO_4 , the intensity of the IR absorption band at 439.7 cm^{-1} on the spectrum of the pyrite dramatically decreased. This absorption band was due to the vibration of the disulfide (S-S) in the lattice of pyrite; the decrease in intensity of this band strongly confirms the presence of the coating on pyritic surfaces. Three additional bands at 1624.3, 1184.7, and 1156.7 cm^{-1} and a broad band ranging from 3700 to 2800 cm^{-1} were also observed on the spectrum of the FePO_4 -coated pyrite (Fig. 7A). The absorption band at 1624 cm^{-1} and the absorption hump around 3000 cm^{-1} are attributable to the bending vibration and rotation of water molecules either adsorbed on iron phosphate or within the structure of iron phosphate. The adsorption bands at 1184.7 and 1156.6 cm^{-1} are due to the P-O internal stretching vibration of PO_4 group (Nanzyo, 1986). Comparison of the spectra of FePO_4 -coated pyrite and amorphous iron phosphate indicates that the iron phosphate coating is most likely amorphous material (Fig. 7A and 7C). However, the slight splitting of the P-O stretching vibration band at 1168 cm^{-1} suggests the tendency of iron phosphate coatings to become crystalline.

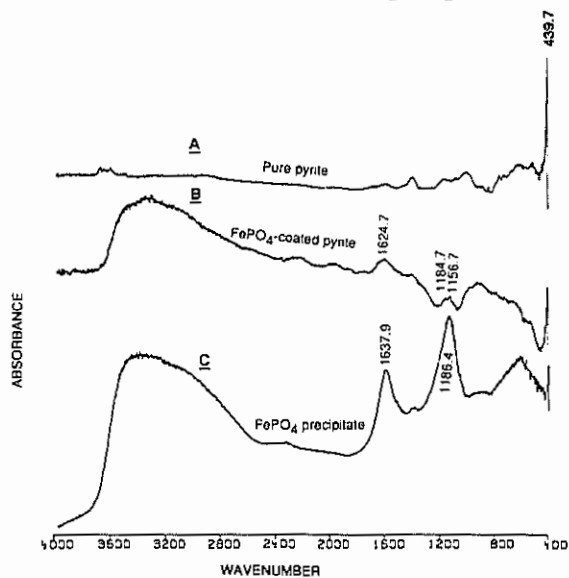


Figure 7. Infrared spectra of A, pyrite; B, FePO_4 -coated pyrite and C, FePO_4 precipitate.

Effectiveness of the FePO_4 Coating in Preventing Pyrite Oxidation

We further tested the feasibility of this coating approach in preventing pyrite oxidation with the pulverized pyritic shale (the sample from which the pure framboidal pyrite was separated). We first leached the shale sample (500 mg) with 500 mL of a solution containing 0.053 mol/L H_2O_2 and 10^{-4} mol/L KH_2PO_4 . This coating process consumed approximately 10% of the total amount of pyrite in the pyritic shale. The pyritic shale was then subjected to leaching with 0.088 mol/L H_2O_2 to test the effectiveness of the coating in preventing pyrite oxidation. As shown in figure 8, after leaching with 0.088 mol/L H_2O_2 for 800 min, only 15% of pyrite in the coated pyritic shale was oxidized, as opposed to more than 80% of pyrite oxidized in the uncoated pyritic shale. This result strongly suggests that the iron phosphate coatings can effectively protect pyrite from oxidizing.

Conclusions

The results of this study demonstrate that an amorphous iron phosphate coating can be established on the surfaces of pyrite in mining "waste" by leaching with a phosphate solution containing H_2O_2 and that the iron phosphate coating could

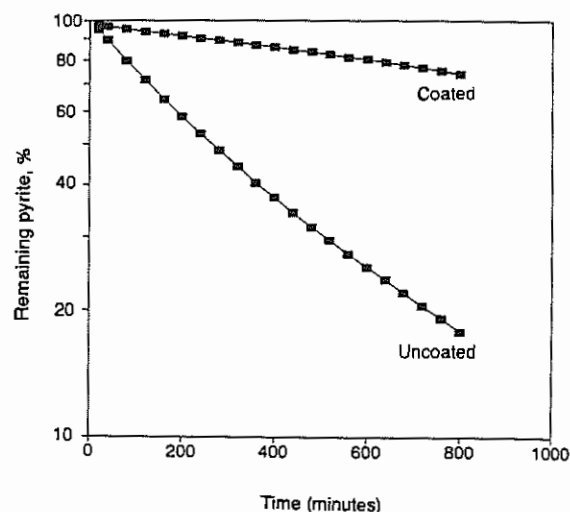


Figure 8. The plot of $\log(100 \times M/M_0)$ versus t for the data of pyrite oxidation when the uncoated and coated pyritic shale samples were leached with 0.088 mol/L H_2O_2 .

effectively prevent pyrite oxidation.

The above conclusion sheds light on a possible solution to the long-unsolved problem of acid mine drainage. This coating approach or technology, if finally extended into practical use, has the following advantages over other approaches. First, due to the permanence of iron phosphate coatings on pyritic surfaces, pyrite particles in mining "waste" can no longer be oxidized and release acid; thus the prevention of the production of acid mine drainage could be permanent. Second, this coating approach does not require the physical mixing of coal wastes with ameliorants and thus can greatly simplify the operation. Third, the coating approach involves using only low concentrations of phosphate and hydrogen peroxide and can dramatically decrease the costs incurred in the operation.

The conclusions drawn in this study are mainly based on the small column experiments, where the effect of the acid produced during leaching with the coating solution on formation of iron phosphate coatings was minimized. It is expected that if we use the coating solution to leach large piles of coal "waste," the pH and concentrations of H_2O_2 and phosphate will decrease as the coating solution goes through the coal wastes. It has been proven in our laboratory that decreases in concentrations of H_2O_2 and phosphate will not significantly influence the efficiency of the coating solution. Nevertheless, the decrease in pH can pose a severe problem; when the pH of the coating solution drops below 4 or to 2, the solution no longer serves as a coating solution but becomes an oxidizing solution. Therefore, it seems essential to introduce a buffer in the coating solution to maintain the pH and the efficiency of the coating solution. Currently, in our laboratory, we are developing a coating solution with an optimal concentration combination of H_2O_2 , KH_2PO_4 , and a buffer reagent to prevent coal wastes from producing acid drainage.

Literature Cited

- Singer, P.C. and W. Stumm. 1970. Acid mine drainage: the rate-determining step *Science* 167:1121-1123.
<http://dx.doi.org/10.1126/science.167.3921.1121>
- Silverman, M.P. 1967. Mechanisms of bacterial pyrite oxidation *J. Bacteriology* 94:1046-1051.
- Nordstrom, D.K. 1982. Aqueous pyrite oxidation and the consequent formation of secondary iron minerals. p. 46-53. In L.R. Hossner, J.A. Kittrick, and D.F. Fanning (eds.), *Acid sulfate weathering: pedogeochemistry and relationship to manipulation of soil minerals*, Soil Sci. Soc. America, Madison, WI.
- Kleinmann, R.L.P., D.A. Crerar, and R.R. Pacelli. 1981. Biogeochemistry of acid mine drainage and a method to control acid formation *Min. Eng.* 3:300-305.
- Ziemkiewicz, P. 1990. Advances in the prediction of and control of acid mine drainage. p. 51-54. In *Proceedings of the Mining and Reclamation Conference and Exhibition*, v 2. Charleston, WV.
<http://dx.doi.org/10.21000/JASMR90010051>
- Ivanov, V.I. 1962. Effect of some factors on iron oxidation by cultures of *Thiobacillus ferrooxidans*. *Microbiology (Engl. Transl.)* 31:645-648.
- Kleinmann, R.L.P., and D.A. Crerar, 1979. *Thiobacillus Ferrooxidans* and the formation of acidity in simulated coal mine environments. *Geomicrobiology J.* 1:373-389.
<http://dx.doi.org/10.1080/01490457909377742>
- Huang, X and V.P. Evangelou. 1992. Abatement of acid mine drainage by encapsulation of acid producing geologic materials. U.S. Bur. Mines Contract j0309013. 60 p.
- Nicholson, R. V., R. W. Gillham, and E. J. Reardon. 1989. Pyrite oxidation in carbonate-buffered solution: 2. Rate control by oxide coatings. *Geochim. Cosmochim. Acta* 54:395-402.
[http://dx.doi.org/10.1016/0016-7037\(90\)90328-I](http://dx.doi.org/10.1016/0016-7037(90)90328-I)
- Turner, R.C. 1960. An investigation of the intercept method for determining the proportion of dolomite and calcite in the mixtures of two. *Can. J. Soil Sci.* 40:232-241.
<http://dx.doi.org/10.4141/cjss60-029>
- Nanzyo, M. 1986. Infrared spectra of phosphate sorbed on iron hydroxide gel and the sorption products. *Soil Sci. Plant Nutri.* 32:51-58.
<http://dx.doi.org/10.1080/00380768.1986.10557480>